arXiv:1704.04692v1 [quant-ph] 15 Apr 2017

Asymptotic Analysis of Coined Quantum Walks on Fractal Networks

Stefan Boettcher and Shanshan Li
Department of Physics, Emory University, Atlanta, GA 30322; USA

We present a detailed analysis of the real-space renormalization group (RG) for discrete-time quantum walks on fractal networks. The RG-flow for such a walk on a dual Sierpinski gasket is obtained explicitly after transforming the unitary evolution equation into Laplace space. Unlike for classical random walks, we find that the long-time asymptotics of the quantum walk requires consideration of a diverging number of Laplace-poles, which we demonstrate exactly for the closed form solution available for the walk on a *1d*-loop. In particular, we calculate the probability of the walk to overlap with its starting position, which oscillates with a period that scales as $N^{d_w^Q/d_f}$ with system size N, consistent with our simulations. While the largest Jacobian eigenvalue λ_1 of the RG-flow merely reproduces the fractal dimension, $d_f = \log_2 \lambda_1$, the asymptotic analysis shows that the second eigenvalue λ_2 becomes essential to determine the dimension of the quantum walk via $d_w^Q = \log_2 \sqrt{\lambda_1 \lambda_2}$. We trace this fact to a delicate cancellation caused by unitarity. We obtain *identical* relations for other networks, although the details of the RG-analysis may exhibit surprisingly distinct features. Thus, our conclusions – which trivially extend to regular lattices – appear to be quite general and likely apply to networks beyond those studied here.

I. INTRODUCTION

Quantum walks [1–5], like random walks before them [6–9], have captured the imagination because of their wide applicability to describe physical situations as well as computational tasks [5, 10–21]. Whether we talk about random or about quantum walks, a complete description for the spreading behavior is provided by the probability density function (PDF) $\rho(\vec{x},t)$ to detect a walk at time t at site of distance $x = |\vec{x}|$ after starting at the origin. For random walks at large times and spatial separations, the PDF obeys the scaling collapse with the scaling variable $x/t^{1/d_w}$,

$$\rho(\vec{x},t) \sim t^{-\frac{d_f}{d_w}} f\left(x/t^{\frac{1}{d_w}}\right), \tag{1}$$

where d_w is the walk-dimension and d_f is the fractal dimension of the network [22]. On a translationally invariant lattice in any spatial dimension $d(= d_f)$, it is easy to show that the walk is always purely "diffusive", $d_w = 2$, with a Gaussian scaling function f. The scaling in Eq. (1) still holds when translational invariance is broken in certain ways or the network is fractal (i.e., d_f is non-integer). However, anomalous diffusion with $d_w \neq 2$ may arise in many of those transport processes [7, 8, 22, 23]. This scaling affects many important observables, for instance, the mean-square displacement, $\langle x^2 \rangle_t \sim t^{2/d_w}$, or first-passage times [24–26].

Elucidating the effects of geometry and internal symmetries on large-scale dynamics is exactly the task that the real-space renormalization group (RG) has been invented for [27], making RG a good method to explore the asymptotic scaling of a walk [8, 22, 24]. Indeed, the RG of classical random walks provides a straightforward blueprint for developing the RG for a quantum walk, even with the added complication of an internal coin space [28]. In this way, exact RG-flow equations for quantum walks on a number of complex networks have been derived [29, 30]. Those results, for instance, have led to the conjecture that the walk dimension d_w in Eq. (1) for a quantum walk with a Grover coin always is *half* of that for the corresponding random walk, $d_w^Q = \frac{1}{2} d_w^R$ [30]. However, the behavior of quantum walks is complicated by the unitarity constraint on the evolution operator. As this constraint is not necessarily expressed by the RG recursion equations, we have argued previously [31] that implies that the leading contribution in the RG-analysis had to be disregarded to access subdominant terms.

Here, we demonstrate in detail, how the leading-order contribution from the RG-analysis cancels to reveal the true scaling behavior. To this end, we explicitly calculate a unitary observable, the amplitude of a quantum walk at its starting position. As this analysis is conducted conveniently via a Laplace-transform, a central role is assumed by the Laplace-poles of the observables. While in the RG for classical random walks it is usually sufficient to follow a single pole, for the quantum walk we find it necessary to consider a *diverging* number of such poles to facilitate a consistent analysis. In light of this, we show how to interpret the fixed-point analysis of the RG-flow. In particular, we provide an interpretation of eigenvalues of the fixed-point Jacobian. Unlike for the classical case of a random walk [24], the RG-flow for a quantum walk must be at least two-dimensional, to yield two relevant eigenvalues. The largest eigenvalue λ_1 always reflects merely the geometry of the network under consideration by determining its fractal dimension d_f, while the dynamics of the quantum walk in form of its walk dimension d_w depends on the second eigenvalue λ_2, i.e.,

$$d_f = \log_b \lambda_1, \qquad d_w^Q = \log_b \sqrt{\lambda_1 \lambda_2}. \tag{2}$$

These results are obtained for two fractal networks, the dual Sierpinski gasket (DSG) and a Migdal-Kadanoff lattice (MK3) [27, 30], where each arrives at the same con-

clusion in quite distinct fashion, suggesting its generality.

This paper is organized as follows: In the next Sec. II, we describe the coined quantum walk, its Laplace transform, and its implementation by example of the dual Sierpinski gasket. In Sec. III we derive the generic RG-recursion equations for the DSG. In Sec. IV, we obtain the RG-flow for a specific implementation of the quantum walk on DSG with a Grover coin. In Sec. V, we analyze the fixed point of the RG-flow and apply the asymptotic flow to determine the amplitude at the origin of the walk, with some details of the arguments being deferred to the Appendix. In Sec. VI, we compare with the corresponding analysis on a Migdal-Kadanoff lattice. We conclude with a discussion and outlook in Sec. VII.

II. QUANTUM MASTER EQUATIONS

The time evolution of a quantum walk is governed by the discrete-time master equation [5]

$$|\Psi_{t+1}\rangle = \mathcal{U}\,|\Psi_t\rangle \tag{3}$$

with unitary propagator $\mathcal{U}$. With $\psi_{x,t} = \langle x|\Psi_t\rangle$ in the discrete N-dimensional site-basis $|x\rangle$, the probability density function is given by $\rho\,(x,t) = \left|\psi_{x,t}^2\right|$. In this basis, the propagator can be represented as an $N \times N$ matrix $\mathcal{U}_{x,y} = \langle x\,|\mathcal{U}|\,y\rangle$ with operator-valued entries that describe the transitions between neighboring sites ("hopping matrices"). We can study the long-time asymptotics via a discrete Laplace transform,

$$\overline{\psi}_x\,(z) = \textstyle\sum_{t=0}^{\infty}\psi_{x,t}z^t, \tag{4}$$

as $z \to 1^-$ implies the limit $t \to \infty$. So, Eq. (3) becomes

$$\overline{\psi}_x = z\mathcal{U}_{x,y}\overline{\psi}_y + \psi_{x,t=0}. \tag{5}$$

Due to the self-similarity of fractal networks, we can decompose $\mathcal{U}_{x,y}$ into its smallest sub-structure, exemplified by Fig. 1. It shows the elementary graph-let of nine sites that is used to recursively build the dual Sierpinski gasket (DSG) of size $N = 3^g$ after g generations. The master equations pertaining to these sites are:

$$\begin{aligned}
\overline{\psi}_0 &= (M+C)\,\overline{\psi}_0 + A\left(\overline{\psi}_3 + \overline{\psi}_4\right) + \psi_{IC},\\
\overline{\psi}_{\{1,2\}} &= (M+C)\,\overline{\psi}_{\{1,2\}} + A\left(\overline{\psi}_{\{5,7\}} + \overline{\psi}_{\{6,8\}}\right),\\
\overline{\psi}_{\{3,4,5,6,7,8\}} &= M\overline{\psi}_{\{3,4,5,6,7,8\}} + C\overline{\psi}_{\{8,5,4,7,6,3\}}\\
&\quad + A\left(\overline{\psi}_{\{0,3,1,5,2,7\}} + \overline{\psi}_{\{4,0,6,1,8,2\}}\right).
\end{aligned} \tag{6}$$

The hopping matrices A and C describe transitions between neighboring sites, while M permits the walker to remain on its site in a "lazy" walk. The inhomogeneous ψ_{IC}-term allows for an initial condition $\psi_{x,t=0} = \delta_{x,0}\psi_{IC}$ for a quantum walker to start at site $x = 0$ in state ψ_{IC}. (It is tedious but straightforward to generalize the following analysis to an initial condition at arbitrary x.)

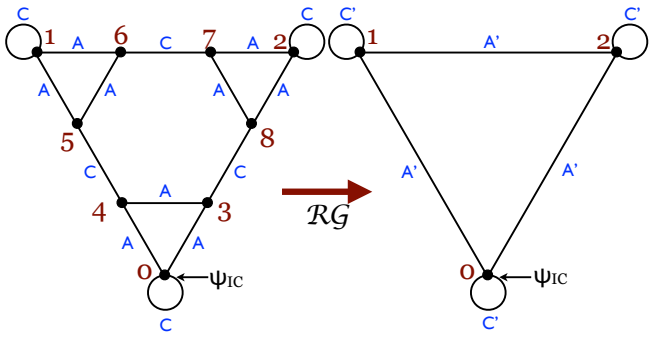

Figure 1. Depiction of the (final) RG-step in the analysis of DSG. The letters $\{A, C\}$ label transitions between sites (black dots on the vertices) of the quantum walk in the form of hopping matrices. (Only on the three outermost sites, the matrix C refers back to the same site.) Recursively, the inner-6 sites (labeled $3, \ldots, 8$) of each larger triangle (left) in DSG are decimated to obtain a reduced triangle (right) with renormalized hopping matrices (primed). To build a DSG of $N = 3^g$ sites, this procedure is applied (in reverse) g times to all triangles at each generation. Note that each generation the base-length L increases by a factor of $b = 2$, such that the fractal dimension is $d_f = \log_{b=2} 3$.

III. RENORMALIZATION GROUP

To accomplish the decimation of the sites $\overline{\psi}_{\{3,\ldots,8\}}$, as indicated in Fig. 1, we need to solve the linear system in Eqs. (6) for $\overline{\psi}_{\{0,1,2\}}$ [32]. Thus, we expect that $\overline{\psi}_{\{3,\ldots,8\}}$ can be expressed as (symmetrized) linear combinations

$$\begin{aligned}
\overline{\psi}_{\{3,4\}} &= P\overline{\psi}_0 + Q\overline{\psi}_{\{1,2\}} + R\overline{\psi}_{\{2,1\}},\\
\overline{\psi}_{\{5,8\}} &= R\overline{\psi}_0 + P\overline{\psi}_{\{1,2\}} + Q\overline{\psi}_{\{2,1\}},\\
\overline{\psi}_{\{6,7\}} &= Q\overline{\psi}_0 + P\overline{\psi}_{\{1,2\}} + R\overline{\psi}_{\{2,1\}}.
\end{aligned} \tag{7}$$

Inserting this Ansatz into Eqs. (6) and comparing coefficients provides consistently for the unknown matrices:

$$\begin{aligned}
P &= (M+A)\,P + A + CR,\\
Q &= (M+C)\,Q + AR,\\
R &= MR + AQ + CP.
\end{aligned} \tag{8}$$

Using the abbreviations $S = (\mathbb{I} - M - C)^{-1}\,A$ and $T = (\mathbb{I} - M - AS)^{-1}\,C$, Eqs. (8) have the solution:

$$P = (\mathbb{I} - M - A - CT)^{-1}\,A,\ R = TP,\ Q = SR. \tag{9}$$

Finally, after $\overline{\psi}_{\{3,\ldots,8\}}$ have been eliminated, we find

$$\overline{\psi}_0 = ([M + 2AP] + C)\,\overline{\psi}_0 + A\,(Q+R)\left(\overline{\psi}_1 + \overline{\psi}_2\right) + \psi_{IC}, \tag{10}$$

and similar for $\overline{\psi}_{\{1,2\}}$ (without ψ_{IC}). By comparing coefficients between the renormalized expression in Eq. (10) and the corresponding, *self-similar* expression in the first

line of Eqs. (6), we can identify the RG-recursions

$$\begin{aligned} M_{k+1} &= M_k + 2A_k P_k, \\ A_{k+1} &= A_k \left(Q_k + R_k\right), \\ C_{k+1} &= C_k, \end{aligned} \tag{11}$$

where the subscripts refer to k- and $(k+1)$-renormalized forms of the hopping matrices. These recursions evolve from the un-renormalized ($k = 0$) hopping matrices with

$$\{M, A, C\}_{k=0} = z\,\{M, A, C\}\,. \tag{12}$$

These RG-recursions are entirely generic and, in fact, would hold for any walk on DSG, classical or quantum. In the following, we now consider a specific form of a quantum walk with a Grover coin.

IV. RG-FLOW FOR THE QUANTUM WALK WITH GROVER COIN

To study the scaling solution for the spreading quantum walk according to Eq. (1), it is sufficient to investigate the properties of the RG-recursion in Sec. III for $\{M, A, C\}$. In the unrenormalized ("raw") description of the walk, these hopping matrices are chosen as

$$M = 0, \quad A = \begin{bmatrix} \frac{1}{2} & 0 & 0 \\ 0 & \frac{1}{2} & 0 \\ 0 & 0 & 0 \end{bmatrix} \mathcal{C}, \quad C = \begin{bmatrix} 0 & 0 & 0 \\ 0 & 0 & 0 \\ 0 & 0 & 1 \end{bmatrix} \mathcal{C}, \tag{13}$$

where at each site A symmetrically shifts weights to two neighboring sites within their local triangle and C shifts weight to the one neighbor outside those triangles, as illustrated in Fig. 1. The walk is not "lazy", i.e., no weight remains at the sites before renormalization, so $M = 0$. These weights are the three complex components of the state vector at each site, $\psi_{x,t}$, which are all zero at $t = 0$, except for $x = 0$ where $\psi_{0,0} = \psi_{IC}$ is arbitrary but normalized, $\left|\psi_{IC}^2\right| = 1$. These weights are entangled at each site before every shift via the unitary 3×3 coin matrix due to Grover, which is given by

$$\mathcal{C} = \frac{1}{3} \begin{pmatrix} -1 & 2 & 2 \\ 2 & -1 & 2 \\ 2 & 2 & -1 \end{pmatrix}. \tag{14}$$

The walk is unitary, i.e., the norm stays preserved, because $\mathcal{C}$ is unitary and $2A + C + M = \mathbb{I}$. Note that $\mathcal{C}$ is also reflective, i.e., $\mathcal{C}^2 = \mathbb{I}$.

Iterating the RG-recursions in Sec. III for the matrices in Eq. (13) for only $k = 2$ steps already reveals a recursive pattern that suggests the Ansatz

$$M_k = \begin{bmatrix} \frac{a_k}{3} + \frac{2b_k}{9} & \frac{a_k}{3} + \frac{2b_k}{9} + \frac{z^2}{z+2} & 0 \\ \frac{a_k}{3} + \frac{2b_k}{9} + \frac{z^2}{z+2} & \frac{a_k}{3} + \frac{2b_k}{9} & 0 \\ 0 & 0 & 0 \end{bmatrix} \mathcal{C}, \tag{15}$$

$$A_k = \begin{bmatrix} \frac{a_k}{3} - \frac{b_k}{9} & \frac{a_k}{3} - \frac{b_k}{9} & 0 \\ \frac{a_k}{3} - \frac{b_k}{9} & \frac{a_k}{3} - \frac{b_k}{9} & 0 \\ 0 & 0 & 0 \end{bmatrix} \mathcal{C}, \qquad C_k = \begin{bmatrix} 0 & 0 & 0 \\ 0 & 0 & 0 \\ 0 & 0 & z \end{bmatrix} \mathcal{C}.$$

Inserted into the RG-recursions in Sec. III, these matrices exactly reproduce themselves *in form* after one iteration, $k \to k+1$, when we identify for the scalar RG-flow:

$$a_{k+1} = \frac{6(z+2)(3z+1)a_k b_k + \left(3z^3 - 5z - 6\right)(3a_k + 2b_k)}{2(z+2)(3z+1)\left(6a_k + b_k\right) + 9\left(3z^3 - 5z - 6\right)},$$

$$b_{k+1} = \frac{\begin{array}{c} 72(z+2)\left(9z^4 - 3z^3 - 9z^2 - z + 6\right) a_k b_k + 12(z+2)(3z+2)\left(3z^3 - 3z^2 + z + 3\right) b_k^2 \\ +36(z+2)^2(9z^2-1)a_k b_k^2 + 9(z+1)\left(3z^3 - 5z - 6\right)\left(3z^2 - 5z + 6\right)(3a_k + 2b_k) \end{array}}{\begin{array}{c} 24(9z^2-1)(z+2)^2 a_k b_k + 4(z+2)^2(9z^2-1)b_k^2 + 27(z+1)\left(3z^3 - 5z - 6\right)\left(3z^2 - 5z + 6\right) \\ +36\left(9z^4 - 3z^3 - 11z^2 - 5z + 6\right)(z+2)a_k + 24(z+2)\left(9z^4 - 3z^3 - 5z^2 + 7z + 6\right) b_k \end{array}}. \tag{16}$$

This flow is initiated at $k = 1$ with

$$\begin{aligned} a_{k=1} &= -\frac{z^2\left(3z^2 + 3z - 2\right)}{(z+2)\left(3z^2 - z - 6\right)}, \\ b_{k=1} &= -\frac{3z^2\left(9z^4 + 12z^3 + 15z^2 + 4z + 12\right)}{(z+2)\left(3z^2 - 5z + 6\right)\left(3z^2 + 5z + 6\right)}. \end{aligned} \tag{17}$$

Note that these RG-flow recursions are vastly simpler than the 5-term recursions previously reported [29].

V. RG-ANALYSIS FOR THE DSG

We now proceed to study the fixed-point properties of the RG-flow at $k \sim k+1 \to \infty$ near $z \to 1$, which builds on the discussion in Ref. [31]. The choice of a_k and b_k in Eq. (15) entails that the Jacobian matrix $\left.\frac{\partial(a_{k+1}, b_{k+1})}{\partial(a_k, b_k)}\right|_{k\to\infty}$ of the fixed point at $z = 1$, $a_\infty = \frac{1}{3}$, and $b_\infty = -2$ already is diagonal, with two eigenvalues, $\lambda_1 = 3$ and $\lambda_2 = \frac{5}{3}$. The eigenvalues correspond to those

two of the five eigenvalues found in Ref. [29] that are relevant, i.e., they are > 1. Extending the expansion of Eq. (16) in powers of $\zeta = z - 1$ for $k \to \infty$ to higher order, we obtain:

$$\begin{aligned} a_k(z) &\sim \frac{1}{3} + \zeta \mathcal{A} \lambda_1^k + \zeta^2 \alpha_k^{(2)} + \zeta^3 \alpha_k^{(3)} + \dots, \\ b_k(z) &\sim -2 + \zeta \mathcal{B} \lambda_2^k + \dots, \end{aligned} \tag{18}$$

with unknown constants $\mathcal{A}$ and $\mathcal{B}$, and with

$$\begin{aligned} \alpha_k^{(2)} &\sim \left(\mathcal{A}\lambda_1^k\right)^2 + \dots, \\ \alpha_k^{(3)} &\sim \left(\mathcal{A}\lambda_1^k\right)^3 + \frac{1}{6}\left(\mathcal{A}\lambda_1^k\right)^2 \left(\mathcal{B}\lambda_2^k\right) + \dots, \end{aligned} \tag{19}$$

where we have only kept leading-order terms in k that contribute in the following considerations.

For the case of a classical random walk, only the dominant eigenvalue λ_1 would be relevant to determine $d_w^R = \log_2 \lambda_1$ [24]. In contrast, in Ref. [31] it was conjectured that for a quantum walk the Jacobian eigenvalues provide d_f and d_w^Q as given in Eq. (2). Here, we shall scrutinize that claim in more detail and show explicitly how to calculate both exponents. Central to this argument is the fact that the observable $\rho(x,t) = \left|\psi_{x,t}^2\right|$ in Eq. (1) has Laplace-poles that only move with k on the unit circle in the complex z-plane, while those poles of a_k and b_k move both tangentially *and* radially on the outside of that circle. That radial motion with k – absent in $\overline{\rho}(x,z)$ – depends only on λ_1, while the tangential motion is controlled by $\sqrt{\lambda_1 \lambda_2}$. This conclusion was based on modeling the behavior of just the two complex poles closest to $z = 1$. Although these conclusions turn out to be correct, a more detailed analysis shows that actually $o(N)$ of such poles impinging on $z = 1$ must be considered here! This we can demonstrate rigorously in Appendix VIII A for the case of a quantum walk on the *1d*-line. Here, we will utilize the implications of that discussion for our analysis of DSG.

Instead of $\overline{\rho}(x,z)$ in its entirety, we focus merely on $\overline{\psi}_0(z)$, the amplitude at the origin of the quantum walk on DSG. According to Fig. 1 and Eq. (10), we have

$$\begin{aligned} \overline{\psi}_0 &= (M_k + C_k)\,\overline{\psi}_0 + A_k\left(\overline{\psi}_1 + \overline{\psi}_2\right) + \psi_{IC}, \\ \overline{\psi}_{\{1,2\}} &= (M_k + C_k)\,\overline{\psi}_{\{1,2\}} + A_k\left(\overline{\psi}_0 + \overline{\psi}_{\{2,1\}}\right), \end{aligned} \tag{20}$$

which has the solution $\overline{\psi}_0 = X_k \psi_{IC}$ with

$$X_k = \left[\mathbb{I} - M_k - C_k - 2A_k\left(\mathbb{I} - M_k - A_k - C_k\right)^{-1} A_k\right]^{-1}. \tag{21}$$

Inserting Eqs. (15) and (18) and expanding (some generic component of) the matrix X_k in powers of $\zeta = z - 1$ yields

$$\begin{aligned} [X_k]_{11} &\sim -\zeta^{-1}\frac{1}{12\left(\mathcal{A}\lambda_1^k\right)} + \zeta^0\left[\frac{11}{12} + \frac{\alpha_k^{(2)}}{12\left(\mathcal{A}\lambda_1^k\right)^2}\right] \\ &\quad + \zeta^1\left[\frac{\left(\mathcal{A}\lambda_1^k\right)\alpha_k^{(3)} - \left(\alpha_k^{(2)}\right)^2}{12\left(\mathcal{A}\lambda_1^k\right)^3} + \frac{5}{72}\left(\mathcal{B}\lambda_2^k\right)\right] + \dots, \\ &\sim \zeta^{-1} O\left(\frac{1}{\lambda_1^k}\right) + \zeta^0 O(1) + \zeta^1 O\left(\lambda_2^k\right) + \dots. \end{aligned} \tag{22}$$

It is the cancellation of the leading $O\left(\lambda_1^k\right)$-term at order ζ^1 that signals the anticipated placement of the Laplace-poles onto the unit circle in the complex z-plane, as demanded by unitarity. As argued in Ref. [31], λ_1 controls the radial movement of poles with k which is removed by this cancellation, thereby exposing λ_2^k as the relevant contribution that controls the tangential movement of poles purely on the unit-circle. Numerical studies of the Laplace-poles of X_k for small values of k, shown in Fig. 2, suggests that these poles arise along arcs on the unit-circle, located symmetrically around the real-z axis due to the real-valued coin such as $\mathcal{C}$ in Eq. (14), and that these poles get increasingly dense and impinge on the real-z axis at $z = 1$. This picture is borne out by our analysis of a quantum walk on the *1d*-loop in Appendix VIII A, which suggests the following generalized form for the amplitude matrix at the origin:

$$\begin{aligned} [X_k]_{11} &\sim \frac{1}{h(N)} \sum_{j=-h(N)}^{h(N)} \frac{f_j}{1 - z\, e^{i\theta_k j g_j}}, \\ &\sim -\zeta^{-1}\frac{f_0}{h(N)} + \zeta^0 \frac{2S_0(N)}{h(N)} - \zeta^1 \frac{4S_2(N)}{\theta_k^2 h(N)} + \dots, \end{aligned} \tag{23}$$

where we defined the sums

$$S_m(N) = \sum_{j=1}^{h(N)} \frac{f_j}{(g_j j)^m}. \tag{24}$$

By analogy with the *1d*-loop, we expect by the fact that the coin in Eq. (14) is reflective and real that both f_j and g_j are real, symmetric, and weakly-varying functions of j (but not N). In turn, $h(N)$ specifies how many Laplace-poles effectively contribute to the asymptotic behavior. If only one (or few) poles contribute, $h(N) = O(1)$, as in the classical case [24], then $S_m = O(1)$ for all $m \geq 0$, and the ζ^0-terms between Eqs. (22) and (23) are inconsistent. The only consistent choice entails that a diverging number of poles must be considered, $h(N) \gg 1$, specifically: $h(N) \sim \lambda_1^k = N$. This implies that (a) $S_0 = O(N)$ and (b) $S_{m \geq 2} = O(1)$. For instance, in the *1d* quantum walk, we have $f_j = g_j = const$ such that both (a) and (b) are satisfied. Matching the expansion also between the ζ^1-terms of Eqs. (22) and (23), we obtain $\theta_k^2 h(N) \sim \lambda_2^{-k}$ or $\theta_k^2 \sim \lambda_1^{-k}\lambda_2^{-k}$. With $L = 2^k$ and assuming that the

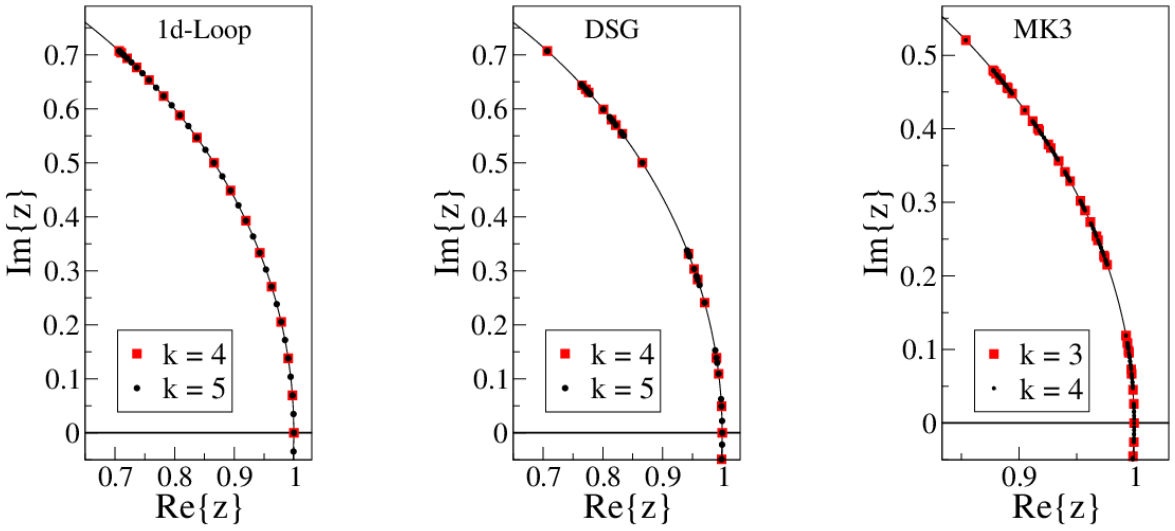

Figure 2. Plot of the poles of the Laplace transforms for the amplitude to remain at the origin, $\overline{\psi}_0^{(k)}(z) = X_k \psi_{IC}$, in the complex-$z$ plane at two consecutive RG-steps k for a quantum walk on the $1d$-line (left), DSG (middle), and MK3 (right). (In these walks, poles are certain to occur in complex-conjugate pairs, so only the upper z-plane is shown.) Although the pattern by which poles evolve appears more complicated for DSG and MK3, a diverging number of those poles progressively impinge on the real-z axis for all systems.

scaling solution implied by Eq. (1) arises via the cut-off at $\theta_k t \sim 1$ [24], i.e., $\theta_k \sim L^{-d_w^Q}$, we arrive at Eq. (2). Expanding to two more orders in powers of ζ provides further prove of the consistency of this interpretation.

The backwards Laplace-transform of X_k in Eq. (23) provides for some typical component in the spinor $\psi_{0,t}$ in a DSG of size $N = 3^k$ that

$$\psi_{0,t} \sim \frac{1}{h\,(N)} \sum_{j=0}^{h(N)} f_j \cos\left(\frac{j g_j t}{N^{d_w^Q/d_f}}\right). \qquad (25)$$

Note that due to condition (a), we have $\left|\psi_{0,t}^{(k)}\right| \sim 1$ for $t = 0$, as would be expected for a walk starting at $x = 0$.

VI. RG-ANALYSIS FOR MK3

To demonstrate the generality of our conclusions, we present briefly also the corresponding analysis for another fractal network, based on the Migdal-Kadanoff hierarchical lattices [27, 33]. The RG-recursions, as depicted in Fig. 3, for this case have already been presented in detail previously in Ref. [30]. Again, all matrices can be parametrized with merely two scalars, most conveniently in the form $\{A, B, C\} = \frac{a+b}{2}\left(P_{\{1,2,3\}} \cdot \mathcal{C}\right)$ and $M = \frac{a-b}{2}\left(\mathbb{I} \cdot \mathcal{C}\right)$, where the $3x3$-matrices $[P_\nu]_{i,j} = \delta_{i,\nu}\delta_{\nu,j}$ (with $\sum_{\nu=1}^{3} P_\nu = \mathbb{I}$) facilitate the shift of the ν-th component to a neighboring site. The RG-flow was found to close for

$$a_{k+1} = \frac{\begin{array}{c}-9a_k + 5a_k^3 + 9b_k + 3a_k b_k - 17a_k^2 b_k - 3a_k^3 b_k \\ +3b_k^2 + 14a_k b_k^2 - 3a_k^2 b_k^2 - 18a_k^3 b_k^2\end{array}}{\begin{array}{c}-18 - 3a_k + 14a_k^2 + 3a_k^3 - 3b_k - 17a_k b_k \\ +3a_k^2 b_k + 9a_k^3 b_k + 5b_k^2 - 9a_k^2 b_k^2\end{array}},$$

$$b_{k+1} = \frac{\begin{array}{c}-3a_k - a_k^2 + 3b_k + 4a_k b_k - 3a_k^2 b_k \\ -b_k^2 + 3a_k b_k^2 + 6a_k^2 b_k^2\end{array}}{\begin{array}{c}6 + 3a_k - a_k^2 - 3b_k + 4a_k b_k \\ +3a_k^2 b_k - b_k^2 - 3a_k b_k^2\end{array}}, \qquad (26)$$

with $a_0 = b_0 = z$. Remarkably, it can be shown that $|a_k| = |b_k| \equiv 1$ for all k, in principle reducing the RG parameters to just two real phases for a_k, b_k.

Similar to DSG in Sec. V, we have a fixed point at $z = 1$ with $a_\infty = b_\infty = 1$. Again, the Jacobian already is diagonal with the two eigenvalues, $\lambda_1 = 7$ and $\lambda_2 = 3$. As before, extending the expansion of Eq. (16) in powers of $\zeta = z - 1$ for $k \to \infty$ to higher order, we obtain:

$$\begin{aligned} a_k\,(z) &\sim 1 + \zeta \mathcal{A} \lambda_1^k + \zeta^2 \alpha_k^{(2)} + \zeta^3 \alpha_k^{(3)} + \ldots, \\ b_k\,(z) &\sim 1 + \zeta \mathcal{B} \lambda_2^k + \zeta^2 \beta_k^{(2)} + \zeta^3 \beta_k^{(3)} + \ldots, \end{aligned} \qquad (27)$$

with unknown constants $\mathcal{A}$ and $\mathcal{B}$, and with

$$\begin{aligned} \alpha_k^{(2)} &\sim \frac{1}{2}\left(\mathcal{A}\lambda_1^k\right)^2 + \ldots, \quad \alpha_k^{(3)} \sim \frac{1}{4}\left(\mathcal{A}\lambda_1^k\right)^3 + \ldots, \\ \beta_k^{(2)} &\sim \frac{1}{2}\left(\mathcal{B}\lambda_2^k\right)^2 + \ldots, \quad \beta_k^{(3)} \sim -\frac{3}{80}\left(\mathcal{A}\lambda_1^k\right)\left(\mathcal{B}\lambda_2^k\right)^2 + \ldots, \end{aligned} \qquad (28)$$

where we have only kept leading-order terms in k relevant for the following considerations.

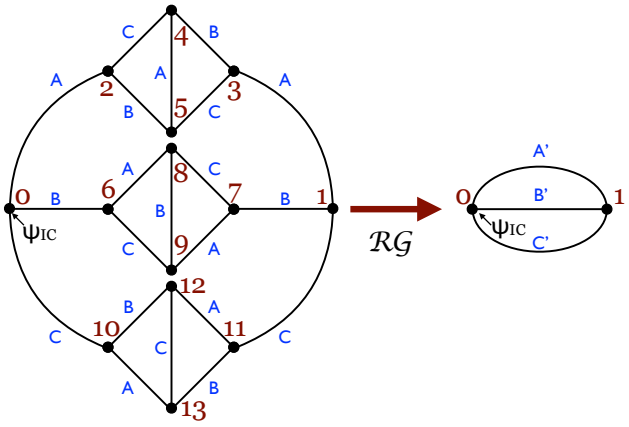

Figure 3. Graphic depiction of the (final) RG-step in the analysis of MK3. The letters $\{A, B, C\}$ label transitions between sites (black dots on the vertices) of the quantum walk in the form of hopping matrices. Recursively, the inner-4 sites (here labeled $2-5$,$6-9$, and $10-13$) of each branch in MK3 are decimated to obtain a reduced set of three lines (right) with renormalized hopping matrices (primed). To build MK3 of $N = 2 \times 7^g$ sites, this procedure is applied in reverses g times to all lines at each generation. Note that each generation the base-length L increases by a factor of 4, such that the fractal dimension is $d_f = \log_4 7$.

The final step of the RG, shown on the right of Fig. 3, is given by

$$\begin{aligned} \overline{\psi}_0 &= M_k \overline{\psi}_0 + (A_k + B_k + C_k)\, \overline{\psi}_1 + \psi_{IC}, \\ \overline{\psi}_1 &= M_k \overline{\psi}_1 + (A_k + B_k + C_k)\, \overline{\psi}_0, \end{aligned} \tag{29}$$

which has the solution $\overline{\psi}_0 = X_k \psi_{IC}$ with

$$X_k = \left[\mathbb{I} - M_k - V_k \left(\mathbb{I} - M_k \right)^{-1} V_k \right]^{-1}, \tag{30}$$

abbreviating $V_k = A_k + B_k + C_k$. Inserting $\{A_k, B_k, C_k, M_k\}$ with the RG-flow in Eq. (27) into X_k in Eq. (30) and expanding in powers of $\zeta = z - 1$ yields for the $(1,1)$-component:

$$\begin{aligned} [X_k]_{11} \sim & -\zeta^{-1} \left[\frac{1}{3\left(\mathcal{B}\lambda_2^k\right)} + \frac{1}{6\left(\mathcal{A}\lambda_1^k\right)} \right] + \zeta^0 \left[\frac{1}{4} + \ldots \right] \\ & + \zeta^1 \left[\frac{\left(\mathcal{A}\lambda_1^k\right) \alpha_k^{(3)} - \left(\alpha_k^{(2)}\right)^2}{6\left(\mathcal{A}\lambda_1^k\right)^3} - \frac{23\left(\mathcal{A}\lambda_1^k\right)}{240} + \ldots \right] \\ & + \ldots, \\ \sim & \, \zeta^{-1} O\left(\frac{1}{\lambda_2^k}\right) + \zeta^0 O(1) + \zeta^1 O\left(\lambda_1^k\right) + \ldots . \end{aligned} \tag{31}$$

Although the ζ^1-term exhibits the same cancelation in the first term as in Eq. (22) for the DSG, other terms of order $O\left(\lambda_1^k\right)$ remain, hiding any contributions from λ_2 here. However, the highly peculiar ζ^{-1}-term *also* reverses the role of the eigenvalues, now selecting λ_2 as the dominant contribution over λ_1 there. Comparison with the expected form of X_k in Eq. (23) then leads to an effective number of poles that scales sub-extensive with the system size, $h\,(N) \sim \lambda_2^k = N^{\log_7 3}$. Consistency then also demands that $S_0(N) \sim h(N)$, so that $S_{m\geq 2}(N) = O(1)$. Amazingly, despite the reversal of roles between λ_1 and λ_2, matching the ζ^1-terms again provides $\theta_k^2 \sim \lambda_1^{-k} \lambda_2^{-k}$, which is invariant to this switch. As before, we have expanded to two more orders in powers of ζ and found consistency throughout. Thus, the RG of MK3 again affirms the result in Eq. (2), all differences in the analysis aside.

VII. DISCUSSION

We have provided a comprehensive description of the real-space renormalization group treatment of discrete-time quantum walks. We have referred to the DSG and MK3 as specific examples, but we expect that this procedure also describes other networks. Our procedure is immediately applicable to study the quantum search algorithm with a coin or power-law localization in hierarchical networks, which we will present elsewhere. Especially, our approach opens the door to a systematic consideration of universality classes in quantum walks and search algorithm. For instance, entire classes of coins can be studied, in particular those that might break the symmetries that were essential do establish the current results and the delicate cancellations these require.

Acknowledgements: SB acknowledges financial support from CNPq through the "Ciência sem Fronteiras" program and thanks LNCC for its hospitality. SL is partially supported through the Emory University PERS program.

[1] Y. Aharonov, L. Davidovich, and N. Zagury, Phys. Rev. A **48**, 1687 (1993).
[2] D. A. Meyer, J. Stat. Phys. **85**, 551 (1996).
[3] D. Aharonov, A. Ambainis, J. Kempe, and U. Vazirani, in *Proc. 33rd Annual ACM Symp. on Theory of Computing (STOC 2001)* (ACM, New York, NY, 2001) pp. 50–59.
[4] J. Kempe, Contemporary Physics **44**, 307 (2003).
[5] R. Portugal, *Quantum Walks and Search Algorithms* (Springer, Berlin, 2013).
[6] M. F. Shlesinger and B. J. West, eds., *Random walks and their applications in the physical and biological sciences* (American Institute of Physics, New York, 1984).
[7] G. H. Weiss, *Aspects and Applications of the Random Walk* (North-Holland, Amsterdam, 1994).
[8] B. D. Hughes, *Random Walks and Random Environments* (Oxford University Press, Oxford, 1996).
[9] R. Metzler and J. Klafter, J. Phys. A: Math. Gen. **37**, R161 (2004).
[10] L. K. Grover, Phys. Rev. Lett. **79**, 325 (1997).

[11] G. S. Engel, T. R. Calhoun, E. L. Read, T.-K. Ahn, T. Mancal, Y.-C. Cheng, R. E. Blankenship, and G. R. Fleming, Nature **446**, 782 (2007).

[12] H. B. Perets, Y. Lahini, F. Pozzi, M. Sorel, R. Morandotti, and Y. Silberberg, Phys. Rev. Lett. **100**, 170506 (2008).

[13] A. M. Childs, Phys. Rev. Lett. **102**, 180501 (2009).

[14] A. Schreiber, K. N. Cassemiro, V. Potoček, A. Gábris, I. Jex, and C. Silberhorn, Phys. Rev. Lett. **106**, 180403+ (2011).

[15] C. Weitenberg, M. Endres, J. F. Sherson, M. Cheneau, P. Schauss, T. Fukuhara, I. Bloch, and S. Kuhr, Nature **471**, 319 (2011).

[16] L. Sansoni, F. Sciarrino, G. Vallone, P. Mataloni, A. Crespi, R. Ramponi, and R. Osellame, Phys. Rev. Lett. **108**, 010502 (2012).

[17] A. Schreiber, A. Gábris, P. P. Rohde, K. Laiho, M. Štefaňák, V. Potoček, C. Hamilton, I. Jex, and C. Silberhorn, Science **336**, 55 (2012).

[18] A. Crespi, R. Osellame, R. Ramponi, V. Giovannetti, R. Fazio, L. Sansoni, F. D. Nicola, F. Sciarrino, and P. Mataloni, Nature Photonics **7**, 322 (2013).

[19] K. Manouchehri and J. Wang, *Physical Implementation of Quantum Walks* (Springer, Berlin, 2014).

[20] V. V. Ramasesh, E. Flurin, M. Rudner, I. Siddiqi, and N. Y. Yao, Phys. Rev. Lett. **118**, 130501 (2017).

[21] C. W. Duncan, P. Öhberg, and M. Valiente, Phys. Rev. B **95**, 125104 (2017).

[22] S. Havlin and D. Ben-Avraham, Adv. Phys. **36**, 695 (1987).

[23] J.-P. Bouchaud and A. Georges, Phys. Rep. **195**, 127 (1990).

[24] S. Redner, *A Guide to First-Passage Processes* (Cambridge University Press, Cambridge, 2001).

[25] S. Condamin, O. Benichou, V. Tejedor, R. Voituriez, and J. Klafter, Nature **450**, 77 (2007).

[26] S. Boettcher and B. Gonçalves, Europhysics Letters **84**, 30002 (2008).

[27] M. Plischke and B. Bergersen, *Equilibrium Statistical Physics, 2nd edition* (World Scientifc, Singapore, 1994).

[28] S. Boettcher, S. Falkner, and R. Portugal, Journal of Physics: Conference Series **473**, 012018 (2013).

[29] S. Boettcher, S. Falkner, and R. Portugal, Phys. Rev. A **90**, 032324 (2014).

[30] S. Boettcher, S. Falkner, and R. Portugal, Phys. Rev. A **91**, 052330 (2015).

[31] S. Boettcher, S. Li, and R. Portugal, J. Phys. A **50**, 125302 (2017).

[32] The following procedure is equivalent to that in Ref. [29], but significantly simplified by the assumption of symmetry, $A = B$, among the hopping matrices.

[33] A. N. Berker and S. Ostlund, Journal of Physics C: Solid State Physics **12**, 4961 (1979).

VIII. APPENDIX

A. Analysis of the Quantum Walk on a Line

The renormalization group treatment of the quantum walk on the $1d$-line [28] provides the RG-flow

$$a_{k+1} = \frac{\sin\eta\, a_k^2}{1 - 2\cos\eta\, b_k + b_k^2},$$
$$b_{k+1} = b_k + \frac{(b_k - \cos\eta)\, a_k^2}{1 - 2\cos\eta\, b_k + b_k^2}. \tag{32}$$

But unlike the analog expressions for DSG in Eq. (16) or MK3 in Eq. (26), this RG-flow in fact possesses a closed-form solution for all $N = 2^k$:

$$a_k = \frac{\cos\sigma\, \sin\eta}{\cos(N\nu + \sigma)}, \quad b_k = \cos\eta + i\frac{\sin(N\nu)\sin\eta}{\cos(N\nu+\sigma)}, \tag{33}$$

where $\nu(z)$ and $\sigma(z)$ are determined by matching to the initial flow, $a_1 = z^2\sin\eta$ and $b_1 = z^2\cos\eta$.

Previously, in Ref. [31], the equivalent of Eq. (21) for the amplitude at the starting-site of a quantum walk, $\overline{\psi}_0 = X_k\psi_{IC}$, for the *1d*-line was shown to be:

$$X_k = \left[\mathbb{I} - (A_k + B_k + M_k)\right]^{-1}. \tag{34}$$

Here, the hopping matrices are parametrized as

$$A_k = \begin{bmatrix} a_k & 0 \\ 0 & 0 \end{bmatrix}\mathcal{C},\ B_k = \begin{bmatrix} 0 & 0 \\ 0 & -a_k \end{bmatrix}\mathcal{C},\ M_k = \begin{bmatrix} 0 & b_k \\ b_k & 0 \end{bmatrix}\mathcal{C} \tag{35}$$

after k renormalization steps, with the coin matrix

$$\mathcal{C} = \begin{pmatrix} \sin\eta & \cos\eta \\ \cos\eta & -\sin\eta \end{pmatrix}. \tag{36}$$

Eqs. (33-35) together provide

$$X_k = \frac{\begin{bmatrix} 1 - a_k\sin\eta - b_k\cos\eta & a_k\cos\eta - b_k\sin\eta \\ -a_k\cos\eta + b_k\sin\eta & 1 - a_k\sin\eta - b_k\cos\eta \end{bmatrix}}{1 - 2a_k\sin\eta - 2b_k\cos\eta + a_k^2 + b_k^2}, \tag{37}$$
$$= \begin{bmatrix} \frac{1}{2} & -\frac{\cot\eta}{2} \\ \frac{\cot\eta}{2} & \frac{1}{2} \end{bmatrix} + \frac{\begin{bmatrix} i\cot\eta + \sin\sigma & i - \sin\sigma\cot\eta \\ \sin\sigma\cot\eta - i & i\cot\eta + \sin\sigma \end{bmatrix}}{2\tan\frac{N\nu}{2}\cos\sigma}.$$

In the following, we shall express X_k asymptotically near the RG fixed-point for $\zeta = z - 1 \to 0$ and $N = 2^k \to \infty$ in *three* different ways: (1.) the exact solution, (2.) the presumed expansion in $O(N)$ Laplace poles, and (3.) the expansion of the RG-flow in Eq. (32), which is typically the only form available in non-trivial applications of the RG. The validation of (2.) and (3.) by (1.) demonstrates our contention that, indeed, a number of Laplace poles must be considered that diverges with N to consistently interpret (3.).

1. Exact Solution:

We simplify matters and (w.r.o.g.) set $\eta = \frac{\pi}{4}$ in the following. With $a_1 = b_1 = z^2/\sqrt{2}$ we find from Eq. (33) that

$$\begin{aligned} \sin 2\nu &= i\left(\frac{1}{z^2}-1\right)\sqrt{1+z^4}, \\ \sin\sigma &= i\,z^2. \end{aligned} \tag{38}$$

The expansion of Eq. (33) in powers of $\zeta = z-1$ is now straightforward and results in

$$\begin{aligned} a_k \sim\ & \zeta^0\frac{1}{\sqrt{2}} + \zeta^1\frac{N}{\sqrt{2}} + \zeta^2\frac{N}{2\sqrt{2}} \\ & -\zeta^3\frac{2\,(N-2)\,(N-1)\,N}{3\sqrt{2}} \\ & -\zeta^4\frac{(N-2)\,N\left(3N^2-8N+2\right)}{6\sqrt{2}}\ldots, \\ b_k \sim\ & \zeta^0\frac{1}{\sqrt{2}} + \zeta^1\frac{N}{\sqrt{2}} + \zeta^2\frac{N\,(2N-3)}{2\sqrt{2}} \\ & +\zeta^3\frac{(N-2)\,(N-1)\,N}{3\sqrt{2}} \\ & -\zeta^4\frac{(N-2)\,N\left(4N^2-6N+5\right)}{12\sqrt{2}}+\ldots. \end{aligned} \tag{39}$$

Inserted into Eq. (37), we find for each component of the matrix X_k in Eq. (37):

$$\begin{aligned} [X_k]_{11} = [X_k]_{22} &\sim -\zeta^{-1}\frac{1}{N} + \zeta^0\frac{N-1}{2N} - \zeta^1\frac{2N^2-5}{12N}+\ldots, \\ [X_k]_{12} = -[X_k]_{21} &\sim \zeta^{-1}0 - \zeta^0\frac{N-2}{2N} + \zeta^1 0+\ldots. \end{aligned} \tag{40}$$

Note that a larger number of terms in Eq. (39) is needed that could potentially contribute to second order in Eq. (40), due to the singular nature of X_k. However, to leading order in N in X_k, those terms finally do cancel.

2. Expansion in Laplace-Poles:

The long-range asymptotics (in space and time) of X_k is determined by its Laplace-Poles in the complex z-plane [31]. As shown in Fig. 2, unitarity demands that these poles are all located on the unit-circle there, and we can parametrize them as $z_j = e^{i\omega_j}$. With $a_1 = b_1 = z^2/\sqrt{2}$ we find from Eq. (38) on the unit-circle:

$$\sin\nu_j = -\sqrt{2}\sin\omega_j, \quad \sin\sigma_j = i\,e^{2i\omega_j}. \tag{41}$$

To find the Laplace-poles of X_k in the second line of Eq. (37), we can ignore the first (non-singular) matrix and focus on the N-dependent zeros of the denominator of the second,

$$\nu_j = \frac{2\pi}{N}j \sim -\sqrt{2}\omega_j, \qquad (j\in\mathbb{Z}), \tag{42}$$

in accordance with Fig. 2. Note, again, that such a result, $\omega_j = j\theta_k$ with

$$\theta_k = \frac{\sqrt{2}\pi}{N}, \tag{43}$$

can only be obtained because we are in possession of the closed-form solution of the RG-flow. It will be the purpose of the next Sec. VIII A 3, and of the entire RG-analysis generally, to produce the scaling of the cut-off in time, $1/\theta_k$, with system size N.

At small ω_j, we also have from Eq. (41) that $\sin\sigma_j \sim i - 2\omega_j$ and $\cos\sigma_j \sim \sqrt{2}$. To evaluate the residue of X_k at the j^{th} pole, we obtain

$$R_j = \lim_{z\to e^{i\omega_j}}\left(z-e^{i\omega_j}\right)X_k \sim -\frac{1}{N}\begin{bmatrix} 1 & -i\omega_j \\ i\omega_j & 1\end{bmatrix} \sim -\frac{1}{N}\,\mathbb{I}, \tag{44}$$

to leading order. Using $\omega_j = j\theta_k$, we then express (some component of) X_k in terms of $h(N) = O(N)$ of such poles,

$$X_k \sim \sum_{j=-h(N)}^{h(N)}\frac{R_j}{z-e^{i\theta_k j}}, \tag{45}$$

$$\begin{aligned} [X_k]_{11} &\sim -\zeta^{-1}\frac{1}{N} - \frac{1}{N}\sum_{j=1}^{h(N)}\left[\frac{1}{\zeta+1-e^{i\theta_k j}} + \frac{1}{\zeta+1-e^{-i\theta_k j}}\right], \\ &\sim -\zeta^{-1}\frac{1}{N} - \frac{1}{N}\sum_{j=1}^{h(N)}\left[\zeta^0 + \zeta^1\frac{2}{\theta_k^2 j^2}+\ldots\right], \\ &\sim -\zeta^{-1}\frac{1}{N} - \zeta^0\frac{h(N)}{N} - \zeta^1\left(\sum_{j=1}^{h(N)}\frac{1}{j^2}\right)\frac{2}{N\theta_k^2}+\ldots. \end{aligned}$$

The last line must be compared with the exact result in Eq. (40). The first term fits exactly, and the last term does fit with the correct choice of θ_k in Eq. (43) and the realization that the sum is always finite, whether $h(N)$ is small or divergent. The key observation concerns the middle term: There, the comparison demands that $h(N) \sim N$, i.e., that we must sum over $O(N)$ poles to make the match consistent. We thus conjecture this to be generically true. In fact, the application of this conjecture allows us to consistently interpret the results for DSG (and other networks).

3. RG-Flow Solution:

Typically, such as for the case of DSG in Eq. (16) or MK3 in Eq. (26), we do not possess a closed-form solution of the RG-flow like Eq. (33). In those cases, we would proceed as in Sec. IV to obtain the asymptotic expansion of the RG-flow by expanding around the fixed point at $z = 1$. This expansion [28] finds the Jacobian eigenvalues

$\lambda_1 = \lambda_2 = 2$ to first order and continues to yield:

$$\begin{aligned} a_k(z) &\sim \frac{1}{\sqrt{2}} + \zeta\mathcal{A}\lambda_1^k + \zeta^2\alpha_k^{(2)} + \zeta^3\alpha_k^{(3)} + \dots, \\ b_k(z) &\sim \frac{1}{\sqrt{2}} + \zeta\mathcal{B}\lambda_2^k + \zeta^2\beta_k^{(2)} + \zeta^3\beta_k^{(3)} + \dots, \end{aligned} \tag{46}$$

with

$$\begin{aligned} \alpha_k^{(2)} &\sim \frac{1}{\sqrt{2}}\left(\mathcal{A}\lambda_1^k\right)^2 - \frac{1}{\sqrt{2}}\left(\mathcal{B}\lambda_2^k\right)^2 + \dots, \\ \alpha_k^{(3)} &\sim \frac{1}{3}\left(\mathcal{A}\lambda_1^k\right)^3 - \frac{5}{3}\left(\mathcal{A}\lambda_1^k\right)\left(\mathcal{B}\lambda_2^k\right)^2 + \dots, \\ \beta_k^{(2)} &\sim \sqrt{2}\left(\mathcal{A}\lambda_1^k\right)\left(\mathcal{B}\lambda_2^k\right) + \dots, \\ \beta_k^{(3)} &\sim \frac{4}{3}\left(\mathcal{A}\lambda_1^k\right)^2\left(\mathcal{B}\lambda_2^k\right) - \frac{2}{3}\left(\mathcal{B}\lambda_2^k\right)^3 + \dots. \end{aligned} \tag{47}$$

Inserting Eq. (46) into the first line of Eq. (37) yields:

$$\begin{aligned} [X_k]_{11} = [X_k]_{22} \sim -\zeta^{-1}\frac{\mathcal{A}+\mathcal{B}}{\sqrt{2}\,\lambda_{1,2}^k\left(\mathcal{A}^2+\mathcal{B}^2\right)} + \zeta^0\frac{1}{2} \\ -\zeta^1\frac{\lambda_{1,2}^k\left(\mathcal{A}+\mathcal{B}\right)}{6\sqrt{2}} + \dots, \\ [X_k]_{12} = -[X_k]_{21} \sim \zeta^{-1}\frac{\mathcal{A}-\mathcal{B}}{\sqrt{2}\,\lambda_{1,2}^k\left(\mathcal{A}^2+\mathcal{B}^2\right)} - \zeta^0\frac{1}{2} \\ +\zeta^1\frac{\lambda_{1,2}^k\left(\mathcal{A}-\mathcal{B}\right)}{6\sqrt{2}} + \dots, \end{aligned} \tag{48}$$

where we have kept only terms to leading order in large $\lambda_{1,2}^k$ for each order of ζ. With the (global) exact solution in Eq. (39), we can easily identify $\mathcal{A} = \mathcal{B} = \frac{1}{\sqrt{2}}$, however, a (local) asymptotic analysis does not provide such information. Thus, we would not realize the accidental cancelation of the $\zeta^{\pm 1}$-terms in the off-diagonal elements of X_k in Eq. (48). As those terms are appearing only as divergent as the ones on the diagonal, it will not affect the conclusions.

In summary, RG would tell us that each component of X_k has the form

$$[X_k]_{ij} \sim \zeta^{-1}O\left(\lambda_{1,2}^{-k}\right) + \zeta^0 O(1) + \zeta^1 O\left(\lambda_{1,2}^k\right) + \dots. \tag{49}$$

Thus, by comparing the ζ^{-1}-term between Eq. (49) and the expected form of the amplitude in Eq. (45), we determine $h(N) \sim \lambda_{1,2}^k = N$. This allows us to conclude that $\log_2\lambda_1 = d_f$, based on the fact that this relation has been observed on all networks studied thus far. This relation may seem obvious from $\lambda_1^k = 2^k$ but could well have be a mere coincidence. (For example, it would be wrong to conclude generally that $\log_2\lambda_2$ provides d_f!) Furthermore, by comparing the ζ^1-terms provides that $\lambda_{1,2}^k \sim 1/\left(N\theta_k^2\right)$, i.e, that the temporal cut-off scales as $\theta_k \sim \lambda_{1,2}^{-k} \sim 1/N$, which implies by Eq. (1) that $d_w^Q = \log_2\lambda_{1,2} = 1$. Note, though, that our main conclusion here is that by comparing order ζ^0-terms we *must* assume $h(N) \sim N$ for a consistent interpretation, i.e., $O(N)$ such poles contribute to this result to make Eq. (49) consistent with the corresponding expansion of Laplace-poles in Eq. (45). Luckily, we do not need to know anything *about* those poles.